pagepress

Journal of Agricultural Engineering

Journal of Agricultural Engineering 2026; LVII:1769
doi:10.4081/jae.2025.1769

Smart precision agriculture using deep neural networks and multi-objective optimization for sensor deployment and yield estimation

Hamdan Alshehri, Haitham Assiri

Department of Computer Science, Jazan University, Saudi Arabia

Abstract

The rapid advancements in communication technologies have initiated transformative changes across various sectors, significantly improving efficiency and quality of life. In the agricultural domain, the growing global demand for food and the need to reduce farmers' workload have positioned the Internet of Things (IoT) as a critical enabler of smart farming solutions. However, accurate prediction of variations in climate conditions, soil attributes, and ground characteristics remains a major challenge in agricultural IoT, with direct implications on crop yield if not effectively addressed. This study proposes an intelligent predictive model for the deployment of IoT sensors in precision agriculture using deep learning techniques. A modified Lemurs optimization (MLO) algorithm is used to predict environmental conditions accurately, enhancing the temperature- humidity-agriculture-meteorology (THAM) index. IoT sensor deployment is optimized using a deep pulse-coupled neural network (DPC-NN) to determine the optimal number and positioning of sensors, ensuring effective coverage of the target agricultural field while improving communication efficiency. The production yield rate is estimated based on key attributes such as fertilizer regulation, temperature quotient, and agronomic factors, optimized using the chaos distributed gravitational search (CDGS) algorithm. Model performance is validated using test samples obtained from the Meteorology Bureau via integrated sensor middleware. Experimental validation using real-world data from the Bureau of Meteorology and Phenonet confirms the robustness. The proposed model achieves yield prediction accuracy of 90.509% with temperature sensors and 90.831% with soil sensors, improves monitoring efficiency to 96.699% in heterogeneous IoT deployments, and surpasses existing benchmark models with a maximum accuracy of 94.6%, RMSE of 0.27, and MAE of 0.21. These results highlight the model's potential to deliver scalable, real-time, and resource- efficient solutions for next-generation precision agriculture.

Key words: precision agriculture; IoT sensor; node deployment; environmental condition; production yield rate.

Correspondence: Hamdan Alshehri, Department of Computer Science, Jazan University, Saudi Arabia. E-mail: halshehri@jazanu.edu.sa

Introduction

It is expected that the world's population would continuously rise throughout the next thirty-five years, accomplishing ten billion people (Devaraj *et al*., 2024). Since the 1980s, when it was initially utilized, precision farming (Pokhrel and Choi, 2024). has transformed how farms work. It does this with the help of instruments like remote detection, Geographic Information Systems (GIS), and Global Positioning Systems (GPS). Artificial Intelligence (AI) and Internet of Things (IoT) sensors work together to makes precision farming (Saini *et al*., 2024). Also, precision farming has made crops more predictable and more resistant to climate change by making them change less often, which is the biggest economic benefit (Lin *et al*., 2023). In the previous 30 years, precision farming has changed a lot. It used to be based on satellite pictures for strategic surveillance to help arrive at choices at the regional level. Now, it leverages low-altitude data from spacecraft to keep an eye on and regulate small field-scale operations (Anand *et al*., 2023). Using technology like ground IoT sensing, remote sensing, satellites, and UAVs (Singh SP *et al*., 2023), as well as incorporated data and data mining, could change the way farming is done, making it more efficient, productive, and long-lasting. Farmers can see their fields in real time and make smart choices about how to grow their crops through submitting sensor data to a central hub over a wireless link (Li *et al*., 2023; Pamuklu *et al*., 2023). Smart farming is good for the digital economy because it creates new markets, is more open, and fixes problems (Martin *et al*., 2024). Smart farming employs AI and the Internet of Things (IoT) to make decisions based on data that help farms work better and get more done (Vangala *et al*., 2022; Pamuklu *et al*., 2022; Chen *et al*., 2022). A lot of research has demonstrated that the Internet of Things (IoT) can keep a watch on things like the temperature, the moisture level in the soil, and the growth of crops all the time. This gets rid of challenges that old-fashioned farming techniques have to deal with (Jeribi *et al*., 2025). They can do this with affordable electronic devices and technology for communication (Sayyad *et al*., 2024). IoT has made it possible to build and update accurate maps of noise, air quality, water pollution, radiation levels, and the weather in real time (Akilan and Baalamurugan, 2024). In precision agriculture that employs the IoT, machine learning (ML) and deep learning (DL) are crucial methods for turning raw data from many sensors into meaningful information. The primary objective of this work is to develop an intelligent predictive model for IoT sensor deployment in precision agriculture using DL techniques. The fol-

lowing is a summary of this work's major contributions:

i) The modified Lemurs optimization (MLO) algorithm is used to predict environmental conditions accurately, thereby enhancing the THAM index.
ii) Optimization of IoT sensor deployment using the deep pulse coupled neural network (DPC- NN) to compute the optimal amount of devices required for comprehensive coverage of the agricultural field, thereby improving communication efficiency.
iii) Calculation of production yield rates, incorporating factors such as fertilizer regulation, temperature considerations, and agronomic variables. These factors are optimized using the chaos distributed gravitational search (CDGS) algorithm.
iv) Validation of the proposed model's performance using test samples obtained from the Meteorology Bureau via the associated sensor middleware.

The remainder of this paper is organized as follows: a review of the existing literature on IoT-based precision agriculture using DL techniques; a section describing the proposed methodology, including environmental condition prediction, optimal IoT node deployment, and the optimization of the production yield rate.

Related work

Several intelligent techniques have been proposed for enhancing IoT-based precision agriculture. While these studies offer significant insights, various limitations persist, which this research aims to address. DL-based irrigation level prediction method using smart IoT was proposed by employing the AHC-ShuffleNetV2 model (Xu *et al*., 2024). The system uses sensor data and images to predict irrigation levels. However, the model's performance may degrade with limited or noisy input data, and it does not address long-term adaptability or generalizability under changing field conditions. An intelligent nonlinear decision tree-based closed-loop control system was used to predict dissolved oxygen levels using the M5 model tree, which achieved a correlation of 0.877 and MAE of 0.963 (Singh M *et al*., 2023). While effective for this specific task, the model's adaptability across diverse environmental parameters remains untested. An intelligent irrigation planning and monitoring system utilizing IoT and LoRa-based ML was developed, resulting in 46% water savings and improved plant health (Lakshmi *et al*., 2023). The study, however, focuses more on energy efficiency and less on predictive accuracy under dynamic weather patterns. A region-based clustering algorithm (REAN) was proposed to enhance energy efficiency in agricultural IoT networks (Priyanka *et al*., 2023). Although the approach improves energy conservation, it lacks discussion on data accuracy or real-time responsiveness. A cloud-integrated smart irrigation system was proposed to connect small-scale farms and aggregate data centrally (Et-taibi *et al*., 2024). While it facilitates scalability, the method not sufficiently addresses issues of sensor placement optimization or communication latency. Another study explored using weather prediction services in a real-world solar-powered test bed to optimize irrigation during rainfall (Irwanto *et al*., 2024). The method is context-specific and lacks generalizability to broader agricultural scenarios with diverse weather unpredictability. An energy- efficient IoT-based framework utilizing adaptive mud ring optimization (AMR) for cluster head (CH) selection and energy-conserving K-means for cluster formation was introduced (Ara *et al*., 2024). The model is effective in network longevity but does not address multi-modal data fusion or predictive analytics. ML model combining improved quantum whale optimization and PCA (IQWO- PCA) was developed to detect tomato diseases (Sowmiya and Krishnaveni, 2023). Deep neural networks such as DenseNet121, AlexNet, ResNet50, and VGG16 were used for feature extraction. However, this approach does not handle real-time processing challenges or integration with irrigation systems. STSDaMaS was proposed to train a neural network for predicting optimal harvesting and baling of forage legume crops (San Emeterio de la Parte *et al*., 2023). While it enhances harvesting prediction, the model is not scalable for multi-crop or multi-environment settings. A scalable IoT architecture was used to remotely monitor and control tractor engines, providing real-time location and status (Shrivastava *et al*., 2023). Though beneficial for equipment monitoring, the model lacks a broader integration with environmental data and decision support for farming activities. The CYPA framework introduced IoT-enabled precision agriculture using decision trees, causal forests, and extra trees, achieving high accuracy (0.9814) (Talaat, 2023). However, the model does not address data inconsistencies or variability in sensor inputs. The WSN performance was evaluated using the 6LowPAN and RPL routing protocols for low-power and lossy networks (Atalla *et al*., 2023). While communication efficiency is improved, the system's capability for intelligent decision- making and prediction is minimal. An IoT-based fertilizer recommendation system was developed using sensor-collected data, with machine learning used for timing and quantity prediction (Kollu *et al*., 2023). Despite excellent accuracy (99.3%), the study lacks clarity on real-time adaptability and robustness to diverse environmental changes. A decision tree-based system achieved 99.2% accuracy for smart fertilizer scheduling (SFSS MLR), showing balanced precision and recall (Abdullahi *et al*., 2024). However, high performance is dataset-dependent, and its generalizability to varied crops and environments is uncertain. An agricultural intelligent decision-making system evaluated the THAM index for node stipulation and the A(t,n) sensor selection method to assess soil humidity and water quality (Mekala *et al*., 2024). Though sensor selection is optimized, the model does not incorporate intelligent learning for adaptive decision-making.

Problem definition

Despite numerous advancements in IoT-enabled precision agriculture, several critical challenges remain unaddressed. As discussed in Table 1, many existing models focus on specific tasks such as irrigation prediction (Xu *et al*., 2024), disease detection (Sowmiya and Krishnaveni, 2023), or fertilizer recommendation (Kollu *et al*., 2023), but lack a unified framework capable of handling diverse agricultural parameters simultaneously. Studies like Sing M *et al*. (2024) and Priyanka *et al*. (2023) highlight the effectiveness of decision tree-based and clustering models, yet fall short in addressing real-time responsiveness and multimodal data integration. While techniques such as transfer learning (Sowmiya and Krishnaveni, 2023) and adaptive optimization (Ara *et al*., 2024) have been employed, they often suffer from high computational costs and limited scalability. Additionally, inconsistencies in sensor data, suboptimal sensor placement, and communication inefficiencies across large field networks continue to hinder system reliability and precision (Atalla *et al*., 2024; Et-taibi *et al*., 2024). Furthermore, the economic and practical feasibility of deploying such intelligent systems in real-world farm settings is often overlooked (Mekala and Viswanathan, 2020; Abdullahi *et al*., 2024). These gaps underscore the need for a scalable, cost-effective, and intelligent predictive model that ensures accurate, real-time, and robust decision-making across heterogeneous agricultural environments.

Table 1. Summary of related works on IoT-based precision agriculture.

Ref.	Methodology	Technique used	Findings	Research gap
Xu *et al.* (2024)	Deep Learning-based irrigation prediction	AHC-ShuffleNetV2 with smart IoT	Predicted irrigation levels using image and sensor data	Does not address adaptability to varying field conditions and real-time feedback
Sing M *et al.* (2023)	Oxygen prediction in water systems	Intelligent nonlinear decision trees (M5 model tree)	Achieved correlation of 0.877 and MAE of 0.963	Limited to a single parameter; lacks multi-sensor integration
Lakshmi *et al.* (2024)	Intelligent irrigation planning	LoRa-based ML with IoT	Reduced water usage by 46%, improved plant health	Lacks adaptability under unpredictable environmental conditions
Priyanka *et al.* (2023)	Energy-efficient IoT clustering	Region-based clustering (REAN)	Improved energy efficiency	No real-time data analysis or prediction capability
Et-taibi *et al.* (2024)	Cloud-based irrigation system	Centralized smart irrigation	Enabled connectivity across farms	Does not optimize sensor placement or data latency issues
Irwanto *et al.* (2024)	Weather-integrated irrigation control	Real-world solar test bed	Improved irrigation during rainfall periods	Not generalizable to other crops or weather patterns
Ara *et al.* (2024)	Energy-efficient IoT architecture	Adaptive Mud Ring Optimization (AMR), K-means	Improved CH selection and energy conservation	No support for multimodal data processing or analytics
Sowmiya and Krishnaveni (2023)	Tomato disease detection	IQWO-PCA, Transfer Learning (DenseNet121, AlexNet, etc.)	Detected tomato disease using image features	No real-time feedback loop; lacks integration with irrigation systems
San Emeterio de la Parte *et al.* (2024)	Crop harvesting prediction	STSDaMaS, Neural Network	Accurate forage legume harvesting predictions	Not scalable to multiple crops or field types
Shrivastava *et al.* (2023)	Equipment control via IoT	Scalable network architecture	Remote monitoring of tractor status and position	Focuses on machinery, not environmental parameters
Talaat (2023)	IoT-based decision-making	CYPA, Decision Trees, Extra Trees	High accuracy (0.9814) in crop analysis	Lacks handling of noisy or inconsistent sensor data
Atalla *et al.* (2023)	Wireless sensor evaluation	6LowPAN with RPL routing protocol	Improved performance in lossy networks	No predictive model or intelligent analytics involved
Kollu *et al.* (2023)	Fertilizer recommendation	ML on IoT sensor data	Achieved 99.3% accuracy	Adaptability to real-time environmental shifts not discussed
Abdullahi *et al.* (2024)	Smart fertilizer scheduling	Decision Tree (SFSS MLR)	Accuracy of 99.2% with balanced F1 metrics	Model performance is highly dataset-dependent
Mekala and Viswanathan method (2020)	Sensor optimization	THAM index, A(t,n) sensor	Evaluated soil and water quality	Lacks intelligent learning and predictive adaptability

Materials and Methods

Figure 1 illustrates the conceptual structure of the proposed intelligent smart predictive model designed for IoT-based precision agriculture. The model focuses on three main components: optimizing the THAM index for effective environmental condition assessment, deploying IoT sensor nodes in optimal positions to ensure maximum field reliable communication, and estimating production yield by analyzing various influencing parameters. This approach divides the agricultural field into zones for zone-specific monitoring and decision-making. Based on their sensing range, sensors are placed to monitor the entire field. This approach considers soil qualities including pH, humidity, temperature, and electricity conductivity, as well as external variables like CO, CO_2, NH_3, and nitrous acid levels. These elements are crucial for agricultural and environmental health. The system helps people make educated choices. Data fusion removes noise and duplicates from incoming data. The system then compares collected data to pre-set threshold values to detect abnormal or critical conditions. After that, statistical categorization classifies situations into alert levels. Finally, real-time SMS or email alerts inform producers or end users of decisions. This methodical approach ensures fast, accurate, and valuable findings, which enhances output and promotes sustainable farming.

Setting up sensors and collecting data

To mimic IoT-based precision agriculture, real-time meteorological data and publicly available datasets were collected. We obtained sensor data from reliable sources like the Bureau of Meteorology (Australia), the Linked Sensor Middleware (LSM) platform, and the Phenonet project, which provides free environmental and phenotyping data. A fake network of 36 sensor nodes depicting various plants or trees was established in agricultural areas ranging from 25x25 m² to 100x100 m². Each node had sensors that assessed soil, ambient, and gas parameters crucial for crop growth and field monitoring. Table 2 shows the set of data and sensor setup. We selected sensors based on soil pH, humidity, temperature, gas focused attention, and electrical conductivity. These parameters affect irrigation planning, disease risk prediction, and output prediction. Data was wirelessly transferred to a Sensor Cloud System for preprocessing, feature extraction, and decision-making. A complete listing of dataset attributes and sensors used in this study is below.

Handling and processing data

A combination of hardware and software architecture managed and analyzed sensor data. Main data collection, preprocessing, fusion, standardization, and first analytical filtering were done in MATLAB R2015. Linked Sensor Middleware (LSM) and storage via the cloud were utilized to collect and handle IoT sensor data streams, comprising humidity, temperature, pH, CO_2, and ammonia levels. Network modeling and deployment optimization were done with a unique tool. This program modeled node deployment in different-sized fields. The obtained data was preprocessed to remove noise, fill values that were missing, and smooth it. The cleansed data were then processed through the proposed intelligent decision-making system, which includes combining information, threshold- based categorization, analytical condition assessment, and stakeholder alarm broadcast. This combined software framework ensured accurate and current precision farming decision assistance.

Predicting the state of the environment

IoT-based precision farming uses the Modified Lemurs Optimization (MLO) method to predict weather. Standard Lemurs algorithm for optimization is improved by this algorithm. It fol-

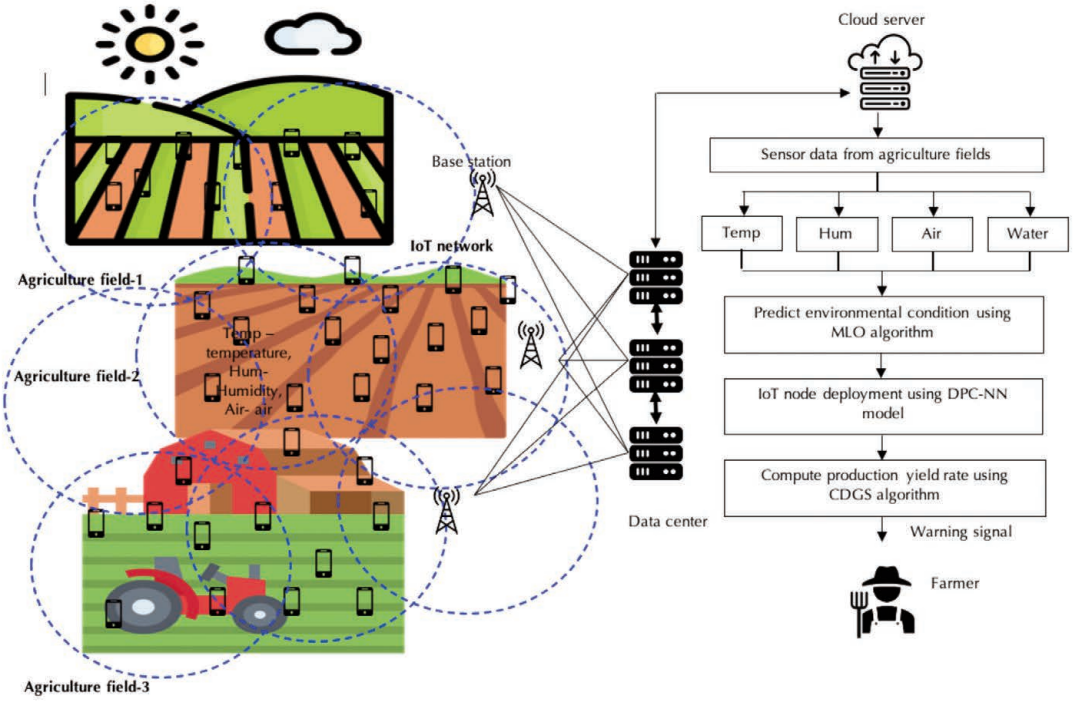

Figure 1. Conceptual structure of proposed model for intelligent smart predictive model for IoT based precision agriculture.

lows how lemurs forage and adapt in complex settings. These features help optimize farming systems affected by environmental changes. The MLO algorithm is crucial for real-time prediction of meteorological components such as soil water content, temperature, transpiration, CO_2 levels, and rainfall in our case study. Incorporating data from nodes of sensors across grid regions, the MLO method offers adaptive prediction that accounts for environmental changes in particular fields. These projections impact crucial farming decisions. For instance:

- Irrigation scheduling can be adjusted to avoid overwatering or drought stress.
- Fertilization timing is optimized based on soil nutrient predictions.
- Pest control measures are aligned with predicted humidity and temperature thresholds.

This predictive capability minimizes waste, conserves water, and increases crop yield. Our implementation of the MLO algorithm treats inputs from sensors as an aggregate matrix, with each individual representing a potential agricultural grid environmental condition. Iterative optimization finds the ideal environment scenario, permitting the decision assistance system to start proactive farming. MLO is strongly coupled with field data to create a sophisticated layer in smart agriculture, integrating conceptual improvement with practical management of crops. MLO algorithm is starting with the initialization process:

$$Z = \begin{bmatrix} k_1^1 & k_1^2 & \cdot & k_1^f \\ k_2^1 & k_2^2 & \cdot & k_2^f \\ \vdots & \vdots & \vdots & \vdots \\ k_m^1 & k_m^2 & \cdot & k_m^f \end{bmatrix} \quad \text{(Eq. 1)}$$

where Z displays the calculation set's lattice in size n d. n concentrates on the applicant arrangements, while d deals with the selection criteria. Define the subsequent parameters for lemurs: Max_iter is the greatest number of iterations, while M is the Populace amount. The dimensionality of the search area over the data set size is implied by f. In addition, the lower bound is denoted by LB and the upper bound by UB. In the u-th solution, generate the Z choice variable as follow:

$$Z_u^h = \left(LB + \left(UB_h - LB_h\right)\right) \times e \quad \text{(Eq. 2)}$$

where e signifies to the unvarying casual amount Z_u^h. Inside the loop estimate the free risk rate (FRR) that is the constant of MLO process.

$$FRR = HRR - y \times \left(\left(HRR - LRR\right) / Max_{iter}\right) \quad \text{(Eq. 3)}$$

where y alludes to the current cycles' amount. Max_{iter} addresses cycle size. Compute the efficiency rating for each *Fit* (Z_u^h) as follows:

$$Fit\left(z_u^h\right) = \alpha \times \left(1 - Acc\right) + \beta \times \left(a / A\right) \quad \text{(Eq. 4)}$$

where the wellness esteem is *Fit* (Z_u^h) little s alludes to the absolute of chosen highlights, A is the greatest chosen component, and Acc

Table 2. Dataset description and sensor configuration.

S.No	Parameter	Sensor type	Measurement unit	Sensor model	Data source	Purpose/usage in model
1	Soil moisture	Capacitive soil moisture sensor	% volumetric water content	VH400 or equivalent	Phenonet, LSM	Irrigation scheduling, water stress detection
2	Soil temperature	Thermistor-based soil sensor	°C	DS18B20 or equivalent	Phenonet	Crop root health analysis, irrigation timing
3	Air temperature	Digital temperature sensor	°C	DHT22	Bureau of Meteorology	Environmental control, yield estimation
4	Humidity	Capacitive humidity sensor	% relative humidity	DHT22	Bureau of Meteorology, Phenonet	Disease risk assessment, evapotranspiration rate
5	Soil pH	Soil pH sensor	pH units	SEN0161	Phenonet	Nutrient management, disease sensitivity analysis
6	Electrical conductivity (EC)	EC sensor	dS/m	Gravity EC sensor	Phenonet, LSM	Soil salinity and fertility evaluation
7	Rainfall	Rain gauge sensor	mm/h	Tipping bucket type	Bureau of Meteorology	Irrigation optimization, weather condition modeling
8	CO_2 concentration	NDIR gas sensor	ppm	MH-Z19	LSM, Phenonet	Crop respiration analysis, greenhouse gas detection
9	CO concentration	Electrochemical gas sensor	ppm	MQ-7	LSM, Phenonet	Pollution monitoring, plant stress indicator
10	Ammonia (NH3) concentration	Semiconductor gas sensor	ppm	MQ-137	LSM	Fertilizer residue tracking, environmental quality
11	Nitrous acid (HONO) level	Chemical sensor (simulated)	ppm	Virtual simulated sensor	Phenonet (Derived)	Nitrogen cycle monitoring, gas emissions analysis

is the precision of every subset. Setting the rating of e1 which is a casual amount (e_3-0.5)x2;$r_1 \leq FRR$ and comparing it with FRR.

$$Z_u^h = \begin{cases} z(u,h) + \left|(z(u,h) - z(bnl,h)\right| \times (e_3 - 0.5) \times 2; r_1 \leq FRR \\ z(u,h) + \left|(z(u,h) - z(bnl,h)\right| \times (e_3 - 0.5) \times 2; r_1 \leq FRR \end{cases} \quad \text{(Eq. 5)}$$

where Z_u^h the casual amount is the current u-th lemur in the Nth Populace; Z° is the competitor arrangement in the h-th decision variable; *z(u,h)* signifies the best lemurs in the world for the entire Populace across all iterations.

$$Z^\circ = \leq z_1^0, z_2^0, z_3^0, \ldots z_u^0 \geq \quad \text{(Eq. 6)}$$

Then, each decision variable $z_u^0 = lb_u + ub_u - z_u$ calculated based on Eq. 7

$$z_u^0 = lb_u + ub_u - z_u \quad \text{(Eq. 7)}$$

where the opposition candidate's upper boundary is lb_u+ub_u the lower boundary. To updates the lemurs' positions within the optimization loop by using the optimal solution as follows:

$$P(ELO) = P(M \times \dim) + P(Max_{iter} \times M) + P(Max_{iter} \times M \times \dim) + P(Max_{Loc-iter}) \quad \text{(Eq. 8)}$$

By improving the accuracy of these predictions, it enhances the THAM index and supports more efficient and effective agricultural management practices. The working process of environmental condition prediction using MLO is depicts in Algorithm 1.

Algorithm 1

Input	: Define the parameter $Max_{Loc-iter}$, dimension d; LRR, and HRR
Output	: Environmental condition
1	Prepare the size of Lemurs populace N.
2	Create populace insouciantly. $Z_u^h = (LB + (UB_h - LB_h)) \times e$
3	Set candidate solutions X
4	Preliminary Lemurs Populace
5	while t <MaxIter do
6	Call Lemurs Process 1 (LO)
7	Apprise lemurs place consuming U-shape or S
8	While Lt <MaxLoc iter do
9	End while
10	End while
11	Reoccurrence an ideal subgroup of feature with advanced exactitude

IoT node deployment

In precision agriculture, the strategic deployment and interconnection of IoT sensor nodes are critical for ensuring efficient data collection, transmission, and environmental monitoring. Each node in the IoT network is equipped with specific sensors that measure environmental parameters such as soil moisture, temperature, humidity, pH, and atmospheric gases. These nodes communicate wirelessly with nearby relay nodes or gateways, forming a mesh network that ensures reliable data transfer to the central monitoring system or cloud-based platform. The signal strength and distance between nodes determine their connectivity. This helps multi-hop transmission protect data in large or irregularly shaped fields. Adaptive routing routes sensor node data packets to the fastest route, reducing delays and energy utilization. This deployment method is improved by a Deep Pulse Coupled Neural Network (DPC-NN). Deep learning and Pulse-Coupled Neural Networks (PCNN), which can handle spatiotemporal data, are used in this model. The DPC-NN considers sensor assortment, overlap, climatic fluctuation, and terrain structure to recommend node locations and connections. DPC-NN ensures that nodes are in the optimum locations to cover the agricultural region and link together in the best method to reduce redundancy and ensure data flow. Environmental monitoring is more reliable and farm managers can make choices faster with this smart deployment. The DPC-NN model has three layers: input, modulation, and pulse generator. We first define the objective function as follows:

$$f_{hg}[b] = T_{hg} \quad \text{(Eq. 9)}$$

where $f_{hg}[b]$ signifies the input of DPC-NN model and T_{hg} signifies the external input stimulus signal and the optimal rating of each input corresponding to the point (h, g).

$$l_{hg}[b] = \sum Z_{hgKL} Q_{KL}[b-1] \quad \text{(Eq. 10)}$$

$$u_{hg}[b] = f_{hg}[b](1 + \beta l_{hg}[b]) \quad \text{(Eq. 11)}$$

$l_{hg}[b]$ is the link input, $u_{hg}[b]$ incomes the internal movement is describes as follows.

$$Q_{hg}[b] = \begin{cases} 1, u_{hg}[b] \geq \theta_{hg}[b] \\ 0, u_{hg}[b] < \theta_{hg}[b] \end{cases} \quad \text{(Eq. 12)}$$

Here $\theta_{hg}[b]$ is the dynamic threshold and $Q_{hg}[b]$ productivity of neurons and displays the gift of connections amid β neurons. When the rating of β is small, the prospect of neighboring neurons firing synchronously is small and we obtain separation outcomes is high. y is used to casually choose which strategy to follow.

$$P(s+1) = \begin{cases} P_{rand}(s) - R_1 \mid P_{rand}(s) - 2R_2 P(s) \mid & y \geq 0.5 \\ P_{rabbit}(s) - \frac{1}{B}\sum_{h=1}^{B} P_h(s) - R_3(lN + R_4(uN - lN)) & y < 0.5 \end{cases} \quad \text{(Eq. 13)}$$

where $P(s)$ refers to the location of hawks presently, $P_{rabbit}(s)$ states to the situation of a rabbit, $P_{rand}(s)$ is the accidental place of one of the existing hawks, P_a is the normal of all hawk situations at the minute, R_1, R_2, R_3, R_4, and y are casual amounts reaching from 0 to 1. In total (uN, lN) mentions to the variety of the preliminary casual position of the hawks.

$$e = 2e_0\left(1 - \frac{s}{S}\right) \quad \text{(Eq. 14)}$$

where is the prey's beginning energy, is its escape energy, and S is the number of repetitions that can occur. The prey attempts to flee when it is in danger; a score of R<0.5 indicates a successful escape, while a score of R>0.5 indicates an unsuccessful attempt at escape. Furthermore, when the besiege is gentle, it occurs at |e| > 0.5, and when it is harsh, it occurs at |e| < 0.5.

$$P(s+1) = \Delta p(s) - e|GP_{rabbit}(s) - P(s)| \quad \text{(Eq. 15)}$$

where $\Delta P(s)=P_{rabbit(s)}$ and G is accidental quantity among 0 and 2.When |e| < 0.5 and R ≥ 0.5, the current place apprises trails:

$$P(s+1) = P_{rabbit}(s) - e|\Delta p(s)| \quad \text{(Eq. 16)}$$

when |e| ≥ 0.5 and R< 0.5, the position apprise is formulate as trails.

$$P(s+1) = \begin{cases} Q \ if \ \ f(Q) < f(P(s)) \\ W \ if \ \ f(W) < f(P(s)) \end{cases} \quad \text{(Eq. 17)}$$

where C and T are the quantities of demand and casual trajectories individually. Levy Flight feature is implemented in status update as follows:

$$\sigma = \left(\frac{\Gamma(1+\beta) \times \sin\left(\frac{\pi\beta}{2}\right)}{\Gamma\left(\frac{1+\beta}{2}\right) \times \beta \times 2^{\frac{\beta-1}{2}}} \right) \quad \text{(Eq. 18)}$$

where u, σ, and v are casual amounts with ratings amid 0 and 1, and β is a non-attendance relentless. When a complex blockade occurs during a progressive rapid dive |e| ≥ 0.5 and R ≥ 0.5 and the Harris Hox level is computed as follows:

$$P(s+1) = \begin{cases} Q \ if \ \ f(Q) < f(P(s)) \\ W \ if \ \ f(W) < f(P(s)) \end{cases} \quad \text{(Eq. 19)}$$

where $Q = P_{rabbit}(s) - e|GP_{rabbit}(s) - P(s)|$ and $W = Q+T$ x $lf(s)$). DPC-NN consist of modules such as coupling strength β, threshold attenuation coefficient α_e:

$$I = -x_1 \times \log_2 x_1 - x_0 \times \log_2 x_0 \quad \text{(Eq. 20)}$$

where x_1 and x_0 characterize the proportion of 0 to 1 in the complete data, individually

$$AH = I(P) + I(Q) - I(P,Q) \quad \text{(Eq. 21)}$$

where I(P) and I(Q) mean bordering entropy of given network information, I(P, Q) rapid the joint solution. The algorithm 2 depicts the working process of IoT node deployment using DPC-NN.

Algorithm 2

Input: Field area, soil parameters, environmental conditions
Output: Node deployment

1. Initialize the casual Populace
2. Define initial objective function $f_{hg}[b] = T_{hg}$
3. If i=0 , j=1
4. While **Do**
5. Compute optimal fitness for fixed length (h, g). $l_{hg}[b] = \sum Z_{hgKL} Q_{KL}[b-1]$
6. Define the initial casual position of the hawks. $e = 2e_0\left(1 - \frac{s}{S}\right)$
7. Compute location update calculation $P(s+1) = P_{rabbit}(s) - e|\Delta p(s)|$
8. Define the optimal threshold to fix the maximum and minimum solution $AH = I(P) + I(Q) - I(P,Q)$
9. End if
10. Update the final rating
11. End

Production yield rate computation

In precision agriculture, production yield rate refers to the measurable output of crops per unit area, influenced by numerous dynamic factors including soil conditions, environmental variables, and farm management practices. Accurate estimation and enhancement of this rate are critical for ensuring sustainable and profitable farming operations. The chaos distributed gravitational search (CDGS) algorithm is employed in the proposed model to improve the factors that have a direct impact on yield. CDGS is a nature-inspired metaheuristic algorithm that uses the global search power of the gravitational search algorithm and the unpredictability of chaos theory to avoid premature convergence and search the solution space more effectively. The method has a hierarchical and distributed structure, which lets it look at many interacting parameters and give better search results that show the best or nearly best circumstances for high crop output. Wheat, rice, and maize are examples of crops that are grown a lot and are used as a reference for theoretical evaluation. These are staple food crops in many agricultural areas and are greatly affected by the environment and soil conditions. The model looks at important factors that affect things like soil pH, moisture content, temperature changes, solar exposure, and nutrient levels. The system's goal is to provide input settings and ambient conditions that will give the highest yield output by optimizing these parameters with the CDGS algorithm. This structured approach helps farmers make data- driven decisions tailored to specific crop categories and environmental setups, ultimately improving productivity, resource utilization, and sustainability in precision agriculture practices. The objective function of prediction model describes as, $P_h = (p_h^l, p_h^l, \ldots p_h^l), h \in \{1,2,\ldots.B\}$, where N represents the total amount of individuals p_h^l and represents its position in the c-th dimension of the search space.

$$a_h(s) = \frac{F_h(s) - F_z(s)}{F_n(s) - F_z(s)} \quad \text{(Eq. 22)}$$

$$A_h(s) = \frac{a_h(s)}{\sum_{L=1}^{B} a_L(s)} \quad \text{(Eq. 22)}$$

Iteration $F_h(s)$ represents the fitness rating in s. $F_z(s)$ and $F_n(s)$ are the worst and best fitness ratings in the iteration, respectively. Lower-level individuals are attracted to middle level higher individuals. CDGS algorithm assumes a sigmoidal gravity constant.

$$J(s) = \frac{J_0}{1 + E^{\frac{s - \frac{S}{2}}{100}}} \quad \text{(Eq. 24)}$$

Gravitational force $p_{hg}^c(s)$ among persons P_h and P_j in the c-th dimension at repetitions is defined as follows.

$$f_{hg}^c(s) = J(s) \frac{A_h(s) \times A_g(s)}{r_{hg}(s) + \varepsilon} \left(p_g^c(s) - p_h^c(s) \right) \quad \text{(Eq. 25)}$$

where $r_{hg}(s)$ is the Euclidean distance among two persons and ε is small continuous. In the middle layer, K best individuals are led by K individual best individuals.

$$n_{hg}^{c}(s)=\frac{rand(-1,1)\cdot\left(x_{hg}^{c}(s)-x_{hg}^{c}(s)\right)}{1+E^{\frac{s-\frac{S}{2}}{100}}} \quad \text{(Eq. 26)}$$

where h ∈K best and g ∈ {1, 2, . . . , CB }. The $n_{hg}^{c}(s)$ c-dimension indicates the update rate of the h-th best individual of g-th sub-Populace in the middle layer. The x_{hg}^{c} c-th dimension represents the h-th unique best individual in the top layer of the j-th sub-Populace.

$$V_{h,g}^{c}(s+1)=Rand_{h,g}\cdot V_{h,g}^{c}(s)+m_{h,g}^{c}(s)+n_{h,g}^{c}(s) \quad \text{(Eq. 27)}$$

where h ∈ {1, 2, . . . , B CB }, g ∈ {1, 2, . . . , CB }. The best individual $p_{n,g}^{c}$ in the j-th sub-Populace replaces the worst individual in the sub-Populace of in all f iterations (g + 1). Personal speed and position $V_{z,g+1}^{c}$ will be updated as follows.

$$V_{z,g+1}^{c}(s+1)=p_{n,g}^{c}(s+1) \quad \text{(Eq. 28)}$$

$$p_{z,g+1}^{c}(s+1)=p_{n,g}^{c}(s+1) \quad \text{(Eq. 29)}$$

Then selects the best individual P_t in the sub-Populace to optimizes the k best individuals in the middle layer. The ideal individual P_t is more directed is more favorable to speed up the convergence of the algorithm. When the historical information P_T is better than the temporary person created in the layer P_t, it changesP_t. The update process is performed as follows:

$$P_{T'}(s)=P_t(s)+x\cdot\left(u_{R2}(s)-u_{R1}(s)\right)\cdot Rand\,(0,1) \quad \text{(Eq. 30)}$$

$$P_t(s)=\begin{cases}P_{T'}(s) & if\ \ F(P_{T'}(s))\le F(P_t(s))\\ P_T(s) & otherwise\end{cases} \quad \text{(Eq. 31)}$$

where x is a constant rating. To perform an experiment to finds the rating of p in the set. u_{R1} and u_{R2} signifies two individuals casually selected from the historical data set. F signifies the fitness function and s is the number of iterations. Then, compute the updated fitness function as follows.

$$n_{hg}^{c}(s)=\frac{rand(-1,1)\cdot\left(x_{T}^{c}(s)-x_{hg}^{c}(s)\right)}{1+E^{\frac{s-\frac{S}{2}}{100}}} \quad \text{(Eq. 32)}$$

The best person in the elite upper layer P_t improves the convergence speed. In the historical data layer, place the individual P_T with the best fitness u_{Max}. If temporary person's fitness is better than u_{Max}, P_t replaces u_{Max}, described as follows.

$$u_{\max}(s)=\begin{cases}P_{T'}(s) & if\ \ F(P_{T'}(s))\le F(P_{Mqx}(s))\\ u_{Max}(s) & otherwise\end{cases} \quad \text{(Eq. 33)}$$

The production yield rate computation using CDGS algorithm involves analysis and optimization of critical agricultural attributes ensures higher efficiency in precision agriculture. Algorithm 3 depicts the working process of production yield rate computation using the CDGS.

Algorithm 3

Input: Soil health, climate conditions, and agricultural practices
Output: Production yield rate

1. Casually initialize B particles
2. **while** the termination criterion is not satisfied do
3. Mass (a) can be created as follows: $a_h(s)=\frac{F_h(s)-F_z(s)}{F_n(s)-F_z(s)}$
4. Define P_h's acceleration $m_h^c(s)$in the c-th|dimension $m_h^c(s)=\frac{f_h^c(s)}{A_h(s)}$
5. Evaluate the fitness
6. for
7. Compute speed and position using hierarchical interactions
$$V_{h,g}^{c}(s+1)=Rand_{h,g}\cdot V_{h,g}^{c}(s)+m_{h,g}^{c}(s)+n_{h,g}^{c}(s)$$
8. end for x
9. If rand > 5.0 then
10. Compute speed and position $V_{z,g+1}^{c}$ will be updated $V_{z,g+1}^{c}(s+1)=p_{n,g}^{c}(s+1)$
11. else
12. Define revised velocity $n_{hg}^{c}(s)=\frac{rand(-1,1)\cdot\left(x_{T}^{c}(s)-x_{hg}^{c}(s)\right)}{1+E^{\frac{s-\frac{S}{2}}{100}}}$
13. End if
14. Compute temporary person's fitness $u_{\max}(s)=\begin{cases}P_{T'}(s) & if\ \ F(P_{T'}(s))\le F(P_{Mqx}(s))\\ u_{Max}(s) & otherwise\end{cases}$
15. Else
16. Update the final rating
17. End

Results and Discussion

This section presents the results and comparative analysis of the proposed and existing models for IoT-based precision agriculture. The MLO+DPC-NN+CDGS model performance is validated using Lenovo PCs equipped with an Intel(R) Core i5-2557M 1.70GHz processor and 4GB RAM. The simulation was conducted using a network simulator tool and MATLAB R2015. Sensor data were obtained from various reliable sources, such as the Bureau of Meteorology, the Linked Sensor Middleware (LSM), and the Phenonet venture. In this study, the IoT network setup consisted of 36 sensor nodes, each representing a tree and equipped with relay nodes, deployed across varying field sizes of 25×25 m², 50×50 m², 75×75 m², and 100×100 m² grids. These sensors primarily focused on monitoring environmental conditions like temperature and humidity, which significantly influence crop growth. However, it is important to note that the findings reported here are specifically influenced by the types of parameters and sensors used in the experimental setup - particularly temperature and atmospheric measurements. For other parameter categories -such as those directly related to soil composition, nutrient content, or specific crop health indica-

Table 3. Threshold for production yield categories.

Class	SO_2	Aqua quality
Low	>0.4	>7.5
Medium	0.2 to 0.4	0.7 to 7.5
High	0 to 0.2	0.5 to 7

Table 4. Threshold for THAM index categories.

Class	THAM index
Normal	<71
Alert	72 to 78
Danger	79 to 81
Emergency	> 82

THAM, temperature-humidity-agriculture-meteorology.

tors- the model performance and threshold outcomes may vary. Hence, while the current setup provides reliable predictions for the considered environmental parameters, further calibration and evaluation would be required when deploying different types of sensors for soil or crop-specific monitoring. The performance of the proposed MLO+DPC-NN+CDGS model was compared with existing models (Mekala and Viswanathan, 2020), including the casual model with THAM (Casual), the opportunity model with THAM (Opportunity), and the optimal (t, n) selection model with THAM ((t, n) selection). Tables 3 and 4 present critical thresholds used for evaluating production yield and environmental alert conditions based on the specific sensor parameters used in this study.

Performance analysis of environmental condition prediction models

The goal is to assess the accuracy of these models in predicting climatic elements including temperature, moisture in the soil, transpiration, CO_2 levels, and rainfall, which significantly affect crop growth and farming operations. The modified Lemurs optimization (MLO) algorithm, particle swarm optimization (PSO), genetic algorithm (GA), and simulated annealing (SA) are being considered. To evaluate each model's agricultural prediction accuracy, processing speed, scalability, and real-time application. Figure 2 compares the effectiveness of four ecological models for prediction (MLO, PSO, GA, and SA) using MAE, RMSE, R^2, and MAPE error measures. The analysis included 10–100 IoT nodes. MLO improved the greatest for MAE, reducing 60% from 0.15 at ten servers to 0.06 at 100 nodes. Similarly, PSO reduced its MAE by 50%, GA by 45% and SA by 40%. The RMSE values also reflected a clear trend of improvement across all models. MLO showed a decrease of 36%, from 0.25 at 10 nodes to 0.16 at 100 nodes. PSO exhibited a 32% reduction, GA improved by 30%, and SA showed a 28% improvement. The decrease in RMSE suggests a more accurate prediction with higher node counts, particularly for the MLO model. In terms of R^2, which indicates the model's ability to explain the variance in the data, all models showed a significant increase in performance as the IoT nodes grew. MLO's R^2 increased by 7%, from 0.92 at 10 nodes to 0.99 at 100 nodes. PSO, GA, and SA showed improvements of 7%, 8%, and 9%, respectively, with PSO going from 0.9 to 0.98, GA from 0.88 to 0.97, and SA from 0.85 to 0.94. MAPE also showed a significant reduction as the number of IoT nodes increased. MLO demonstrated the largest improvement of 47%, decreasing from 4.5 at 10 nodes to 2.4 at 100 nodes. PSO improved by 42%, GA by 35%, and SA by 32%. PSO reduced from 5.2 to 3.1, GA from 6 to 3.9, and SA from

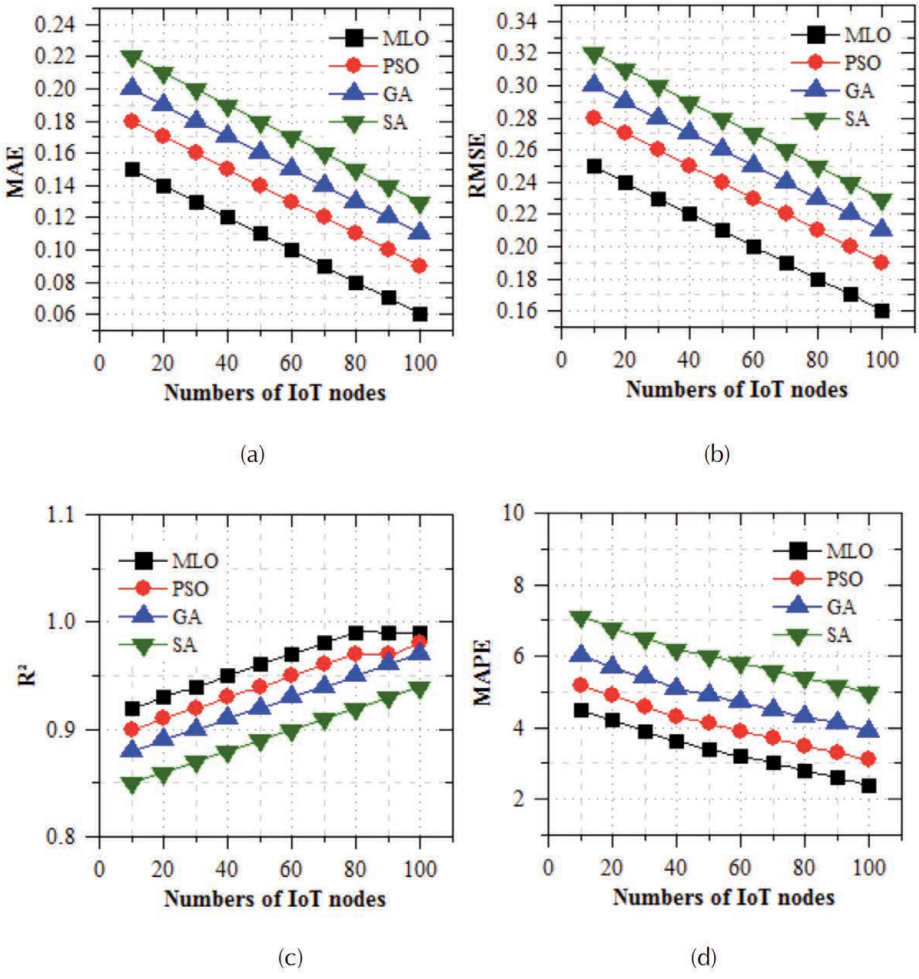

Figure 2. Error metrics analysis for environmental condition prediction models in terms of (**a**) MAE, (**b**) RMSE, (**c**) R^2 and (**d**) MAPE for the IoT-based precision agriculture models.

7.1 to 5. The analysis shows that increasing the number of IoT nodes leads to consistent performance improvements across all models. MLO did better than the other optimization methods in terms of MAE, R^2, and MAPE. The PSO, GA, and SA performed better in terms of RMSE and R^2. These findings demonstrate that adding IoT nodes to precision agriculture systems improves model accuracy and forecast reliability. As shown in Figure 3, the forecasting algorithms (MLO, PSO, GA, and SA) for IoT-based agricultural precision systems performed differently for duration of processing, integration, security, and scalability. When IoT nodes increased from 10 to 100, all models had longer periods of processing and more converging iterations. They gained durability and scalability to varying degrees. MLO had the smallest processing time increase, 120% from 1500 ms at 10 nodes to 3300 ms at 100

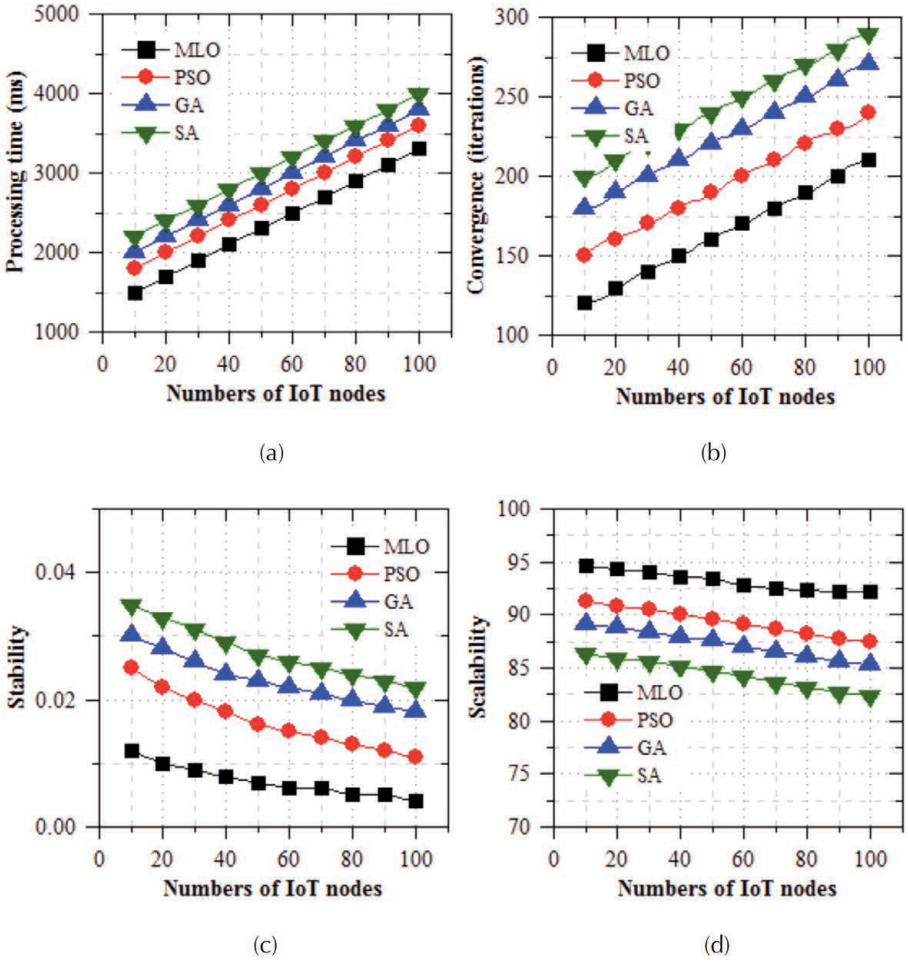

Figure 3. Performance evaluation and scalability analysis of prediction models (**a**) processing time (ms), (**b**) convergence (iterations), (**c**) stability and (**d**) scalability for the IoT-based precision agriculture models.

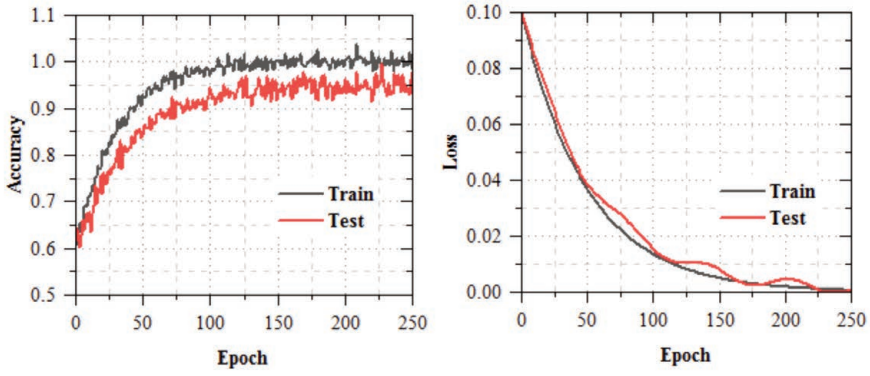

Figure 4. Training and testing performance of proposed DPC-NN model for IoT temperature sensors deployment.

nodes. GA rose 90%, SA 82%, and PSO 100%. These data show that MLO is the fastest at running, whereas SA uses the most resources. When it came to convergence, all of the models revealed that the number of iterations needed generally went up as the number of IoT nodes went up. MLO demonstrated the smallest increase, rising by 75% from 120 to 210 iterations. PSO saw a 60% increase, GA exhibited a 50% rise, and SA showed a 45% increase. This indicates that MLO maintains faster convergence across increasing system complexity. Stability analysis showed significant improvements across all models. MLO showed the largest gain in stability, with its fluctuation value decreasing by 67%, from 0.012 at 10 nodes to 0.004 at 100 nodes. PSO followed with a 56% improvement, GA improved by 40%, and SA showed a 37% improvement. These findings affirm MLO as the most stable model across increasing data sizes. In terms of scalability, represented by R^2 values, all models showed slight decreases as the number of IoT nodes increased. MLO had the smallest reduction in scalability, with a 2.6% decline from 94.58 at 10 nodes to 92.12 at 100 nodes. PSO decreased by 4%, GA by 4.4%, and SA experienced the most significant drop of 4.7%. Despite this, MLO consistently maintained the highest scalability performance. The result illustrates that increasing the number of IoT nodes enhances stability and convergence while increasing processing demand. MLO consistently outperformed the other models in terms of execution time, stability, and scalability, making it the most efficient model for large-scale IoT-based precision agriculture systems. PSO, GA, and SA showed relative improvements in convergence and stability but lagged behind MLO in scalability and processing efficiency.

Comparative analysis of IoT node deployment models

The comparative analysis of various IoT node deployment models in precision agriculture reveals the superior performance of the proposed DPC-NN model, particularly when combined with MLO and CDGS. Figure 4 illustrates the training and testing performance of the DPC-NN model for temperature sensor deployment, showcasing smooth and consistent trends in both accuracy and loss. The training accuracy steadily increases and converges near 99%, while the validation accuracy stabilizes around 91-92%, indicating strong learning capability and generalization. The training loss exhibits a sharp exponential decline, and the validation loss mirrors this trend with minor fluctuations, reflecting model stability and minimal overfitting. Compared to the Casual, Opportunity, and (t, n) selection models, the MLO+DPC-NN+CDGS framework demonstrates significant improvements in sensor selection efficiency, prediction accuracy, and processing time. These enhancements result in better resource optimization and monitoring efficiency, especially in large or heterogeneous agricultural fields. The proposed model proves to be a robust and scalable solution for IoT-based environmental monitoring in precision agriculture.

The performance evaluation in Table 5 shows that the proposed MLO+DPC-NN+CDGS model works well for deploying IoT nodes with temperature sensors, especially when it comes to choosing sensors, getting accurate readings, and processing time. The proposed method cuts the number of selected sensors by 78.26% when 20 IoT nodes are installed, and it keeps cutting the number of sensors by 60% even when there are 100 nodes. This tendency of choosing the best sensors is also clear in the Opportunity model and the (t, n) selection model, where the number of nodes dropped by 70.59% and 54.55%, respectively. The MLO+DPC-NN+CDGS model is always more accurate than other methods. It does 23.28% better than the Casual model, 13.99% better than the Opportunity model, and 6.56% better than the (t, n) selection model at the 100-node setup. This shows that the proposed model has a better learning ability and a better way to optimize sensors. Comparisons of IoT nodes using soil sensors demonstrate that the MLO+DPC-NN+CDGS model is better at sensing productivity, precision, and processing time. The amount of the chosen sensors lowers significantly in the proposed model. It reduces sensor utilization by 46.15% comparable to the (t, n) selecting model, 36.36% comparable to the Opportunity model, and 46.15% comparable to the Casual model with 100 IoT nodes. These reductions are consistent across smaller deployments, demonstrating the system's scalability and resource efficiency. At

Table 5. Result comparison of models for IoT node deployment with temperature sensors.

Model	Amount of IoT nodes				
	20	40	60	80	100
	Amount of selected sensors				
Casual	23	24	26	28	30
Opportunity	17	18	20	22	24
(t, n) selection	11	12	14	16	18
MLO+DPC-NN+CDGS	5	6	8	10	12
	Accuracy (%)				
Casual	72.862	73.089	73.227	74.258	74.630
Opportunity	78.494	78.721	78.859	79.890	80.262
(t, n) selection	84.126	84.353	84.491	85.522	85.894
MLO+DPC-NN+CDGS	89.758	89.985	90.123	91.154	91.526
	Processing time (ms)				
Casual	42000	42500	43000	43500	44000
Opportunity	32000	32500	33000	33500	34000
(t, n) selection	22000	22500	23000	23500	24000
MLO+DPC-NN+CDGS	12000	12500	13000	13500	14000

the 100-node level, the proposed model is 16.92% more accurate than the Casual model, 10.48% more effective than the possibility model, and 4.99% more accurate than the (t, n) selection model. The pattern stays the same for all node sizes, which shows that the model can keep making good predictions even when the deployment gets more complicated. The findings for processing time show even more how efficient the proposed methodology is at doing math. At 100 nodes, it cuts processing time by 68.37% compared to the Casual model, 60.26% compared to the Opportunity model, and 46.55% compared to the (t, n) selection model. The fact that the MLO+DPC-NN+CDGS model consistently improves all major metrics shows that it is a very accurate solution for precision agriculture IoT- based soil monitoring applications. The results in Table 7 show that the MLO+DPC-NN+CDGS model works well to improve measurement rating and monitoring efficiency in IoT-based precision agriculture, even when there are different numbers of deployed nodes. The proposed model constantly does better than other models in terms of measurement rating, no matter what the setup is. With 50 IoT nodes, MLO+DPC- NN+CDGS gets a measurement rating that is 11.54% higher than the Casual model, 9.66% higher than the Opportunity model, and 7.87% higher than the (t, n) selection model. These improvements reflect the model's strong ability to maintain high-quality environmental measurements even as network scale increases. The same trend is evident in monitoring efficiency. At 50 nodes, the MLO+DPC-NN+CDGS model improves monitoring efficiency by 16.01% compared to the Casual model, 11.85% compared to the Opportunity model, and 7.91% compared to the (t, n) selection model. These consistent gains, even with a lower number of IoT nodes, suggest that the proposed model not only enhances the quality of sensor measurements but also ensures optimal sensor network performance. The steady rise in performance with node count indicates strong scalability, making the MLO+DPC-NN+CDGS model a highly effective solution for real-time, resource-efficient agricultural monitoring. The evaluation of IoT-based precision agriculture across varying agricultural field areas, as shown in Table 8, demonstrates the strong performance of the MLO+DPC-NN+CDGS model in both measurement rating and monitoring efficiency. With increasing field

Table 6. Result comparison of models for IoT node deployment with soil sensors.

Model	Amount of IoT nodes				
	20	40	60	80	100
	Amount of selected sensors				
Casual	26	27	31	35	39
Opportunity	20	21	25	29	33
(t, n) selection	14	15	19	23	27
MLO+DPC-NN+CDGS	8	9	13	17	21
	Accuracy (%)				
Casual	77.148	77.549	77.882	78.279	78.412
Opportunity	81.473	81.874	82.207	82.604	82.737
(t, n) selection	85.799	86.200	86.533	86.930	87.063
MLO+DPC-NN+CDGS	90.125	90.526	90.859	91.256	91.389
	Processing time (ms)				
Casual	47000	47500	48000	48500	49000
Opportunity	37000	37500	38000	38500	39000
(t, n) selection	27000	27500	28000	28500	29000
MLO+DPC-NN+CDGS	13500	14000	14500	15000	15500

Table 7. Results of IoT based precision agriculture with varying amount of IoT nodes.

Model	Amount of IoT nodes				
	10	20	30	40	50
	Measurement rating (%)				
Casual	76.685	77.038	77.078	77.288	77.601
Opportunity	78.000	78.353	78.393	78.603	78.916
(t, n) selection	79.316	79.669	79.709	79.919	80.232
MLO+DPC-NN+CDGS	85.632	85.985	86.025	86.235	86.548
	Monitoring efficiency (%)				
Casual	82.689	82.915	83.418	83.559	83.719
Opportunity	85.847	86.073	86.576	86.717	86.877
(t, n) selection	89.005	89.231	89.734	89.875	90.035
MLO+DPC-NN+CDGS	96.128	96.354	96.857	96.998	97.158

sizes from 1 to 5 acres, the proposed model maintains a consistently higher measurement rating than all other models. At 5 acres, it improves measurement rating by 14.32% over the Casual model, 10.04% over the Opportunity model, and 6.05% over the (t, n) selection model. This means that the proposed method works very well to keep sensor data gathering trustworthy, even when the field gets bigger. The MLO+DPC-NN+CDGS model is better in monitoring efficiency than other models in all field sizes. It does 11.67% better than the Casual model, 9.12% better than the Opportunity model, and 6.71% better than the (t, n) selection model at the 5-acre milestone. These results clearly show that the proposed model scales well with field size, which guarantees both high measurement accuracy and the best operating performance. The steady rise in value shows that it is suitable for use in large-scale agricultural monitoring systems where accuracy, scalability, and efficiency are very important.

Results analysis of yield estimation

To test the proposed yield prediction model that combines DPC-NN and CDGS, ten test cases (TC1- TC10) were created with different environmental and agricultural conditions. These scenarios included changes in temperature, humidity, fertilizer amount, and soil wetness to make them more like real-life farms and to test how well the model could predict outcomes with both good and bad inputs. Table 9 shows that the model works quite well when conditions are perfect. The model got very low MAPE values (all below 3%) and R^2 scores above 0.93 in TC2, TC3, TC6, and TC10, where the temperature and humidity were moderate, the fertilizer amounts were medium to high, and the soil moisture was about right. This shows that the model can learn a lot and be very accu-

Table 8. Results of IoT based precision agriculture with varying agriculture field area.

Model	Agriculture field area (acre)				
	1	2	3	4	5
	Measurement rating (%)				
Casual	75.993	76.170	76.403	76.543	76.554
Opportunity	78.978	79.155	79.388	79.528	79.539
(t, n) selection	81.963	82.140	82.373	82.513	82.524
MLO+DPC-NN+CDGS	86.948	87.125	87.358	87.498	87.509
	Monitoring efficiency (%)				
Casual	84.901	84.997	85.066	85.173	85.281
Opportunity	86.886	86.982	87.051	87.158	87.266
(t, n) selection	88.871	88.967	89.036	89.143	89.251
MLO+DPC-NN+CDGS	94.856	94.952	95.021	95.128	95.236

Table 9. Yield estimation accuracy under varying environmental and agronomic conditions using the proposed MLO+DPC-NN+CDGS based model.

Test case	Temp (°C)	Humidity (%)	Fertilizer level	Soil moisture	Actual yield (t/ha)	Predicted yield (t/ha)	MAPE (%)	R^2 score
TC1	32	40	Low	Dry	2.600	2.400	7.692	0.880
TC2	28	65	Medium	Optimal	3.800	3.700	2.632	0.940
TC3	30	70	High	Optimal	4.300	4.200	2.326	0.960
TC4	27	80	Medium	Wet	3.600	3.400	5.556	0.890
TC5	34	45	High	Dry	3.200	2.900	9.375	0.850
TC6	29	75	Medium	Optimal	3.700	3.600	2.703	0.930
TC7	33	55	Low	Optimal	2.900	2.700	6.897	0.870
TC8	26	85	High	Wet	4.100	3.900	4.878	0.910
TC9	35	40	Medium	Dry	2.700	2.400	11.111	0.820
TC10	30	60	High	Optimal	4.400	4.300	2.273	0.960

Table 10. Comparative performance analysis of the proposed model with state-of-the-art techniques in terms of accuracy, RMSE, and MAE for yield prediction in precision agriculture.

Methodology	Accuracy (%)	RMSE	MAE	Accuracy ↑	RMSE ↓	MAE ↓
AHC-ShuffleNetV2 [16]	89.323	0.4298	0.3115	5.931%	-35.741%	-32.264%
LoRa-ML [18]	91.221	0.3863	0.2932	3.733%	-28.954%	-27.594%
IQWO-TL [23]	90.534	0.3658	0.2824	4.539%	-25.004%	-25.001%
MLO+DPC-NN+CDGS (proposed)	94.626	0.2752	0.2175	–	–	–

rate when conditions are good for growing crops. When the conditions were not quite right, such when the soil was a little too dry or too wet or when less fertilizer was used, the predictions were a little less accurate. In TC1, TC4, TC7, and TC8, MAPE went up a little but stayed below safe ranges, between 4.88% to 7.69%. It's important to note that the R^2 values in these test instances were still above 0.87. This shows that the model is strong and can adapt to less-than-ideal situations while still keeping a solid correlation between actual and anticipated yields. Performance dropped more drastically when there was stress. The model indicated higher MAPE values of 9.38% and 11.11% in TC5 and TC9, which both had dry soil with high temperatures or high fertilizer levels. The R^2 scores declined to 0.85 and 0.82, respectively. These results show how important soil moisture is for estimating yield. They also show that the model is sensitive to a lack of moisture, although it still makes a good estimate. On average, the model recorded an R^2 of 0.901 and a MAPE of 5.204%, reflecting consistent predictive capability across all test conditions. These averages confirm that the proposed model delivers high accuracy and generalization, even in challenging environmental conditions. To further validate its performance, Figure 5 shows the actual versus predicted yield values were plotted, showing close alignment with minimal deviation in most cases. Although the model is primarily regression-based, ROC and Precision-Recall curves were also generated by discretizing yield into categories. These classification-oriented metrics reaffirm the model's effectiveness, particularly its ability to maintain precision and recall under varying conditions.

Results comparison between proposed and state-of-art works

The performance comparison presented in Table 10 clearly demonstrates that the proposed Hybrid Deep Learning-IoT Fusion model significantly outperforms existing state-of-the-art methods in terms of accuracy, RMSE, and MAE. The proposed model achieved the highest accuracy of 94.6%, surpassing the AHC-ShuffleNetV2 model (Xu *et al*., 2024) by 5.93%, the LoRa-ML Hybrid model (Lakshmi *et al*., 2023) by 3.73%, and the IQWO-TL-based model (Sowmiya and Krishnaveni, 2023) by 4.53%. This notable improvement in accuracy is attributed to the integration of real-time multimodal IoT sensor data and an advanced deep learning framework that facilitates adaptive feature learning. The use of attention mechanisms and context-aware temporal-spatial modeling allows the system to precisely capture critical variables like temperature, soil moisture, humidity, and fertilizer levels, leading to better decision boundaries. In terms of RMSE, the proposed model recorded a significantly reduced error of 0.27, representing a decrease of 35.71% compared to Xu *et al*. (2024) 28.95% compared to Lakshmi *et al*. (2023), and 25.00% compared to Sowmiya *et al*. (2023). The drop is because to a hybrid loss function, good regularization methods, and a better training approach that uses early halting and noise-filtered input data. The model's flexibility to work in many environments makes sure that the actual and anticipated yields are quite close to each other, which is important for making accurate predictions. The MAE value, which is another important error statistic, is likewise the lowest for the

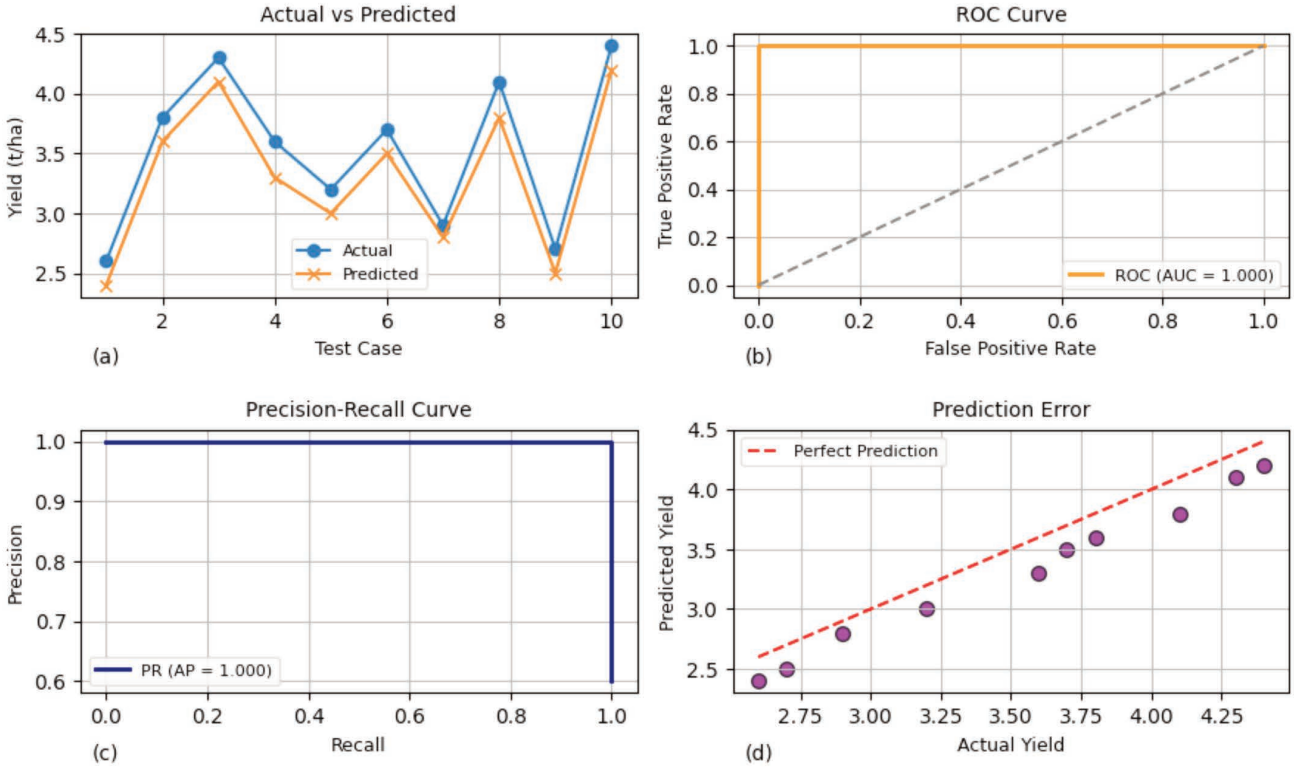

Figure 5. Comprehensive visualization of the proposed yield prediction model's performance (**a**) actual-predicted yield across 10 test cases, demonstrating close alignment in optimal conditions; **b**) ROC curve highlighting the model's binary classification capability with high AUC; **c**) precision- recall curve confirming the model's effectiveness under imbalanced yield classes; **d**) prediction error scatter plot illustrating accuracy with most points clustering around the ideal diagonal line.

proposed model at 0.21. This is a 32.26%, 27.59%, and 25.00% decrease from the models in Xu *et al*. (2024), Lakshmi *et al.* (2023) and Sowmiya and Krishnaveni (2023), respectively. The model's ability to learn in detail, which allows it to pick up on small changes in field-level data and use real-time feedback from IoT inputs, makes this development possible. Also, hyperparameter tuning with grid search and cross-validation techniques makes sure that the predictions are strong and consistent. Table 10 shows that the proposed system's advantages are not only small ones; they come from strategic improvements in both data integration and model architecture. These changes show that hybrid AI-IoT systems could be able to give precision agriculture precise, real-time, and flexible solutions for predicting yields.

Conclusions

By combining deep learning with IoT, this study creates a smart and flexible prediction framework for IoT-based precision agriculture. The proposed method uses a modified Lemurs optimization (MLO) algorithm to provide accurate predictions about important environmental factors. This improves the THAM index for making smart agricultural decisions. A deep pulse-coupled neural network (DPC-NN) is used to make sure that IoT sensors are placed in the best possible way. This helps with sensor allocation and cuts down on redundancy across different field sizes. Using a chaos distributed gravitational search (CDGS) method that optimally weighs agronomic factors including temperature, fertilizer application, and soil moisture improves the yield prediction. We have thoroughly tested the proposed MLO+DPC-NN+CDGS model using simulations and real-world sensor data from trusted sources including the Bureau of Meteorology and Phenonet. The results show that the performance is far better than that of the best models that are currently available:

- The proposed model gets a yield prediction accuracy of 90.509% with temperature sensors and 90.831% with soil sensors. This is an improvement of 12.445% and 9.525%, respectively, over baseline models.
- It gets 96.699% for diverse IoT node deployments and 95.039% for different field areas when it comes to monitoring efficiency. This is 10.632% and 8.386% better than current approaches, respectively.
- The study in Table 10 demonstrates that the proposed hybrid model is better than top-tier alternatives like AHC-ShuffleNetV2, LoRa-ML Hybrid, and IQWO-TL. It has a maximum accuracy of 94.6%, an RMSE of just 0.27, and an MAE of 0.21. These numbers show that the models did better than the best-performing benchmark models by 5.93%, 35.71%, and 32.26%, respectively.

These improvements validate the potential of the proposed model to provide scalable, real-time, and resource-efficient solutions for agricultural monitoring and yield prediction. Consequently, the MLO+DPC-NN+CDGS model presents a robust and deployable system for next-generation precision agriculture, capable of adapting to diverse environmental and field conditions while maintaining high prediction fidelity.

Limitations and future direction

The real-time field deployment could encounter practical challenges such as hardware limitations, sensor failures, or communication delays. In terms of application, the proposed system shows strong potential in supporting herbaceous crop management (such as wheat, maize, and paddy) where yield prediction is crucial for irrigation scheduling and resource optimization. With appropriate tuning, it could also be extended to tree-based perennial crops (e.g., apple, citrus) by integrating remote sensing data and canopy-specific parameters. Future work will focus on enhancing cross-domain adaptability and incorporating more diverse data modalities (e.g., drone imagery, weather APIs) for broader applicability in smart agriculture.

References

Abdullahi, M.O., Jimale, A.D., Ahmed, Y.A., Nageye, A.Y. 2024. Revolutionizing Somali agriculture: harnessing machine learning and IoT for optimal crop recommendations. Discov. Appl. Sci. 6:77.

Akilan, T. ,Baalamurugan, K.M. 2024. Automated weather forecasting and field monitoring using GRU-CNN model along with IoT to support precision agriculture. Expert Syst. Appl. 249:123468.

Anand, G., Vyas, M., Yadav, R.N., Nayak, S.K. 2023. On reducing data transmissions in fog enabled LoRa based smart agriculture. IEEE Internet Things J. 11:8894-890.

Ara, T., Ambareen, J., Venkatesan, S., Geetha, M., Bhuvanesh, A. 2024. An energy efficient selection of cluster head and disease prediction in IoT based smart agriculture using a hybrid artificial neural network model. Measure. Sensors 32:101074.

Atalla, S., Tarapiah, S., Gawanmeh, A., Daradkeh, M., Mukhtar, H., Himeur, Y., et al. 2023. Iot- enabled precision agriculture: Developing an ecosystem for optimized crop management. Information 14:205.

Chen, L.B., Huang, G.Z., Huang, X.R., Wang, W.C. 2022. A self-supervised learning-based intelligent greenhouse orchid growth inspection system for precision agriculture. IEEE Sensors J. 22:24567-24577.

Devaraj, H., Sohail, S., Li, B., Hudson, N., Baughman, M., Chard, K., et al. 2024. RuralAI in tomato farming: Integrated sensor system, distributed computing and hierarchical federated learning for crop health monitoring. IEEE Sensors Lett. 8:1-4.

Et-taibi, B., Abid, M.R., Boufounas, E.M., Morchid, A., Bourhnane, S., Hamed, T.A., Benhaddou, D., 2024. Enhancing water management in smart agriculture: a cloud and IoT-based smart irrigation system. Results Eng. 22:102283.

Irwanto, F., Hasan, U., Lays, E.S., De La Croix, N.J., Mukanyiligira, D., Sibomana, L., Ahmad, T., 2024. IoT and fuzzy logic integration for improved substrate environment management in mushroom cultivation. Smart Agr. Technol. 7:100427.

Jeribi, F., Tahir, A., Rana, N., Ramakrishnan, J., Martin, R.J., 2025. CentralMaizeGuard: Enhanced deep learning model for maize disease detection and management. Arch. Control Sci. 35:221-250.

Kollu, P.K., Bangare, M.L., Hari Prasad, P.V., Bangare, P.M., Rane, K.P., Arias-Gonzáles, J.L., et al. 2023. Internet of things driven multilinear regression technique for fertilizer recommendation for precision agriculture. SN Appl.Sci. 5:264.

Lakshmi, G.P., Asha, P.N., Sandhya, G., Sharma, S.V., Shilpashree, S., Subramanya, S.G. 2023. An intelligent IOT sensor coupled precision irrigation model for agriculture. Measure. Sensors 25:100608.

Li, X., Hou, B., Zhang, R., Liu, Y., 2023. A review of RGB image-based internet of things in smart agriculture. IEEE Sensors J. 23:24107-24122.

Lin, Q., Guo, X., Xie, Y., Peng, K., Yang, R., Cai, K., 2023.

Surface matching-based markerless global optimization registration for improved optical surgical systems in internet-of-things enabled operating rooms. IEEE T. Consum. Electr. 70:939-946.

Martin, R.J., Mittal, R., Malik, V., Jeribi, F., Siddiqui, S.T., Hossain, M.A., Swapna, S.L. 2024. XAI-powered smart agriculture framework for enhancing food productivity and sustainability. IEEE Access 12:168412-168427.

Mekala, M.S., Viswanathan, P. 2020. (t, n): sensor stipulation with THAM index for smart agriculture decision-making IoT system. Wirel. Pers. Commun. 111:1909-1940.

Pamuklu, T., Nguyen, A.C., Syed, A., Kennedy, W.S., Erol-Kantarci, M. 2022. IoT-aerial base station task offloading with risk-sensitive reinforcement learning for smart agriculture. IEEE T. Green Commun. Netw. 7:171-182.

Pamuklu, T., Syed, A., Kennedy, W.S., Erol-Kantarci, M. 2023. Heterogeneous GNN-RL based task offloading for UAV-aided smart agriculture. IEEE Netw. Lett. 5:213-217.

Pokhrel, S.R., Choi, J. 2024. Data-driven satellite communication and control for future IoT: principles and opportunities. IEEE T. Aero. Elec. Sys. 60:3307-3318.

Priyanka, B.H.D.D., Udayaraju, P., Koppireddy, C.S., Neethika, A. 2023. Developing a region- based energy-efficient IoT agriculture network using region-based clustering and shortest path routing for making sustainable agriculture environment. Measure. Sensors 27:100734.

Saini, R., Garg, P., Chaudhary, N.K., Joshi, M.V., Palaparthy, V.S., Kumar, A. 2024. Identifying the source of water on plant using the leaf wetness sensor and via deep learning based ensemble method. IEEE Sens. J. 24:7009-7017.

San Emeterio de la Parte, M., Martínez-Ortega, J.F., Hernández Díaz, V., Martínez, N.L., 2023. Big Data and precision agriculture: a novel spatio-temporal semantic IoT data management framework for improved interoperability. J. Big Data 10:52.

Sayyad, S.B., Shaikh, M.A., Anpat, S.M., Kolapkar, M.M. 2024. IoT based soil monitoring for precision agriculture. In: Lamine S., Srivastava P.K., Kayad A., Muñoz-Arriola F., Chandra Pandey p. (eds.), Remote sensing in precision agriculture. Academic Press. pp. 43-59.

Shrivastava, P., Tewari, V.K., Gupta, C., Singh, G. 2023. IoT and radio telemetry based wireless engine control and real-time position tracking system for an agricultural tractor. Discov. Internet Things 3:6.

Singh, M., Sahoo, K.S., Gandomi, A.H. 2023. An intelligent IoT-based data analytics for freshwater recirculating aquaculture system. IEEE Internet Things J. 11:4206-4217.

Singh, S.P., Dhiman, G., Juneja, S., Viriyasitavat, W., Singal, G., Kumar, N. ,Johri, P. 2023. A new QoS optimization in IoT-smart agriculture using rapid adaption based nature-inspired approach. IEEE Internet Things J. 11:5417-5426.

Sowmiya, M., Krishnaveni, S. 2023. IoT enabled prediction of agriculture's plant disease using improved quantum whale optimization DRDNN approach. Measure. Sensors 27:100812.

Talaat, F.M., 2023. Crop yield prediction algorithm (CYPA) in precision agriculture based on IoT techniques and climate changes. Neural Comput. Appl. 35:17281-17292.

Vangala, A., Das, A.K., Mitra, A., Das, S.K., Park, Y. 2022. Blockchain-enabled authenticated key agreement scheme for mobile vehicles-assisted precision agricultural IoT networks. IEEE

T. Inf. Forens. Secur. 18:904-919.

Xu, X., Patibandla, R.L., Arora, A., Al-Razgan, M., Awwad, E.M., Nyangaresi, V.O. 2024. An adaptive hybrid (1D-2D) convolution-based ShuffleNetV2 mechanism for irrigation levels prediction in agricultural fields with smart IoTs. IEEE Access 12:71901-71918.

Received: 10 March 2025; Accepted: 1 September 2025.

Contributions: all authors made a substantive intellectual contribution, read and approved the final version of the manuscript and agreed to be accountable for all aspects of the work.
Conflict of interest: the authors declare no competing interests, and all authors confirm accuracy.

Acknowledgements: the authors gratefully acknowledge the funding of the Deanship of Graduate Studies and Scientific Research, Jazan University, Saudi Arabia, through Project Number: RG24- S0155.